Theoretical Investigation of Formaldehyde Reactions Initiated by OH Radicals

Gladson de Souza Machado[1], Glauco Favilla Bauerfeldt [*, 1]

[1] Departamento de Química. Universidade Federal Rural do Rio de Janeiro, Brazil

Abstract

The kinetic parameters for the H_2CO + OH reaction are found in the literature with great dispersion, showing high dependence with the level of theory. In this work, in order to clarify the main steps, and the corresponding best kinetic parameters, involved in formaldehyde oxidation mechanism, the elementary reactions are investigated adopting the CCSD(T) method at the complete basis set limit. The set of chemical reactions include: H_2CO + OH → HCO + H_2O (R1), HCO → H + CO (R2), HCO + OH →(E)-CH_2O_2 (R3), (E)-CH_2O_2 → H_2O + CO (R4), (E)-CH_2O_2 → (Z)-CH_2O_2 (R5) and (Z)-CH_2O_2 → H_2 + CO_2 (R6). Canonical variational rate coefficients were also calculated and Arrhenius parameters are recommended.

Introduction

Formaldehyde is found in troposphere, being either emitted from anthropogenic and biogenic sources or formed from the photooxidation of the organic compounds. Among the emission sources, industrial and vehicular exhaustion emissions seem to be the most important contribution to carbonyl compounds levels in the troposphere at urban regions [1-4]. Its chemical removal, besides the photochemical dissociations, is expected to occur by two main channels: the reactions with NO_3 and with OH radicals, the latter expected to prevail since OH radicals are more reactive than the NO_3 [5-7].

From the reactivity point, previous experimental and theoretical kinetic studies have shown that the hydrogen abstraction reaction initiated by OH radical is favored, in comparison to the radical addition reaction [7-8]. Although theoretical works have found values for the rate coefficient in the order of magnitude of 10^{-12} $cm^3 \cdot molec^{-1} \cdot s^{-1}$ for the hydrogen abstraction reaction at atmospheric conditions, there is still a large discrepancy in the values of the reaction barrier height, varying between -1.0 and 5.5 kcal mol^{-1} [9-16].This variation is highly associated with the accuracy of the level of calculation adopted, the most accurate levels associated with the lowest barrier height values.

Moreover, previous works [8,14] have highlighted the importance of a pre barrier complex for this reaction, attributing to it the non-Arrhenius behavior at low temperatures. On the other hand, the increase of rate coefficients at high temperatures has also been reported [13,15,17]. This behavior of the rate coefficient is probably due to a change in the reaction mechanism, although such point, to the best of our knowledge, has not yet been discussed in the literature.

Thus, the main goal of this work is to revisit the mechanism for the oxidation of formaldehyde initiated by OH radicals, using high-level *ab initio* methods, and to calculate the rates coefficients by the variational transition state theory, in order to identify the most important oxidation pathways, at atmospheric and combustion conditions.

Computational Methods

Theoretical calculations were performed at the coupled cluster level, including single and double excitations, and adopting the aug-cc-pVDZ basis set (CCSD/ACCD). The stationary points corresponding to reactants, products, saddle points and pre barrier complex were located and each minimum energy geometry has been further characterized by the vibrational frequencies.

The reaction paths were calculated either from the intrinsic reaction coordinate (IRC) algorithm [18], connecting reactants and products with a reaction path passing through a saddle point, and rigid scans, which connects the reactants and products with a barrierless reaction path.

In order to improve the accuracy of the electronic energies, single point calculations at the CCSD(T)/ACCD level were also performed. Moreover, single point calculations at the second-order Møller-Plesset perturbation theory (MP2) level with aug-cc-pVDZ, aug-cc-pVTZ and aug-cc-pVQZ basis sets (MP2/ACCD, MP2/ACCT and MP2/ACCQ) were also performed in order to estimate the electronic energy at the complete basis set limit (CBS), by:

$$E(n) = E^{\infty} + C_1 \cdot exp(-C_2 \cdot n) \quad (1)$$

$$E_{CCSD(T)/CBS} = E_{CCSD(T)/ACCD} + (E^{\infty} - E_{MP2/ACCD}) \quad (2)$$

Where E(n) are the MP2 electronic energy with the aug-pVnZ, being "n" the numeric value attributed to each basis (ACCD=2, ACCT=3, ACCQ=4) and C1, C2 and E^{∞} are parameters. The latter represents the energy at the complete basis set limit (CBS, $n \rightarrow \infty$). This procedure, applied not only to the minimum energy structures, but also to the non-stationary points along each reaction path, has been widely used to obtain more accurate and reliable electronic energy values [19-21].

The thermal corrections to the internal energy, entropy, enthalpy and Gibbs free energy were calculated according to the standard equations of statistical thermodynamics, adopting rigid rotor, harmonic oscillator and ideal gas models. In this way, it was also

[*] Corresponding author: bauerfeldt@ufrrj.br

possible to transform the reaction path energies from the ground-state vibrationally adiabatic potential curve (*i.e.* the reaction coordinate as a function of the electronic energies corrected by vibrational zero point energies) to the Gibbs free curves, in order to calculate the rates coefficients by the canonical variational transition state method.

Finally, with the calculated rates coefficients, the dynamic behavior of the proposed chemical model has been analyzed at atmospheric condition (T=298 K) and combustion condition (T=1000 K) using the software Kintecus® [22].

Results and Discussion

The chemical model is based on six elementary steps, being the reaction of formaldehyde with OH radicals leading to the formyl radical and water (R1: $H_2CO + OH \rightarrow HCO + H_2O$) the first elementary step of the mechanism, followed by the dissociation of the formyl radical (R2: CHO→CO+H) and further reaction of the formyl radical with OH, leading to formic acid (R3: CHO+OH→(E)-CH_2O_2), which decomposes to carbon monoxide and water (R4: (E)-CH_2O_2→ H_2O+CO) and to molecular hydrogen and carbon dioxide (R6: (Z)-CH_2O_2→H_2+CO_2), after isomerization from the E to Z conformation (R5: (E)-CH_2O_2→(Z)-CH_2O_2). The reactions of this chemical model are exhibited in Figure 1.

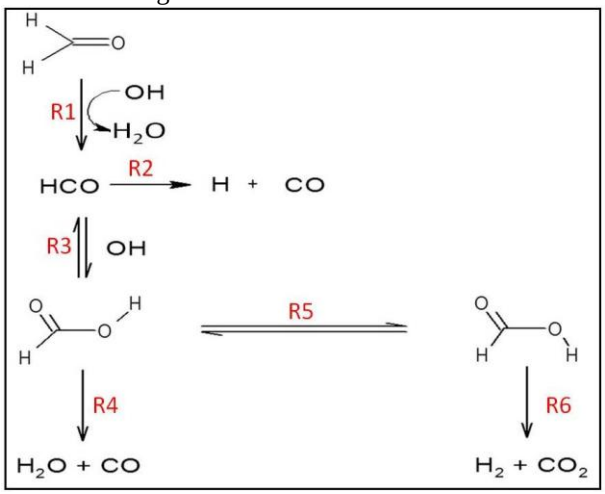

Figure1: Chemical model of the formaldehyde oxidation by OH radicals.

The hydrogen abstraction reaction (R1) proceeds via reversible formation of a prebarrier complex, a structure which is stabilized with respect to the isolated reactants due to hydrogen bond and connects to the products passing through a saddle point. The decomposition of the formyl radical (R2) also proceeds by a typical potential curve, in which saddle point is located. The association reaction (R3) is represented by a barrierless potential curve. Saddle points could also be characterized for all the reactions involving the conformers of the formic acid (R4, R5 and R6). The global reaction profile is introduced in the Figure 2.

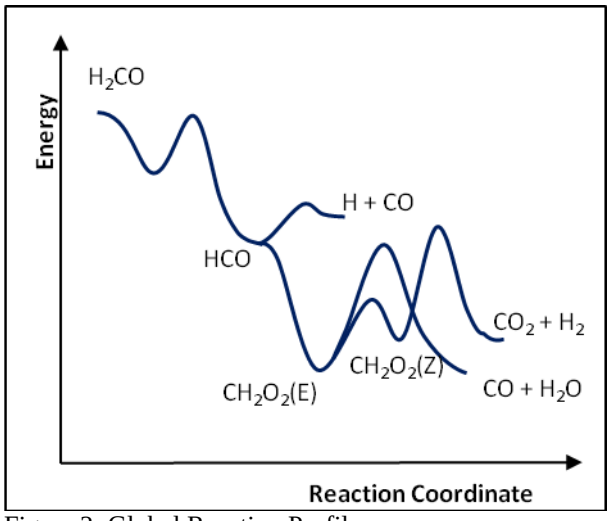

Figure 2: Global Reaction Profile.

The geometric parameters and the vibrational frequencies, calculated for the molecules and radicals at the CCSD/ACCD level, show excellent agreement with the experimental values [23]. The maximum deviation is noted for the formyl radical, the root mean square deviations (rms) for the distances, angle and vibrational frequencies being 0.04 Å, 5 degrees and 164 cm^{-1}, respectively. The rms values correspond to relative deviations of 2.9 %, 4.3% and 5.3% , respectively.

Calculated standard reaction enthalpy values are shown in Table 1 and experimental values are also given for comparison. The improvement of the enthalpy differences values, as a result of the CBS procedure is remarkable. Unfortunately, similar analysis could not be done for the reactions involving the Z conformer of the formic acid, since there is no experimental value of standard enthalpy of formation for this specie.

Table 1: Standard reaction enthalpy values (ΔH^o, in $kcal \cdot mol^{-1}$), obtained at different theoretical levels. Experimental values [23] are included for comparison.

ΔH^o ($kcal \cdot mol^{-1}$)	CCSD/ ACCD	CCSD(T)/ ACCD	CCSD(T)/ CBS	Exp.
R1	-24,42	-25,83	-28,42	-29,02
R2	12,86	12,84	14,87	15,29
R3	-99,89	-101,98	-109,17	-110,21
R4	1,35	2,23	4,63	6,27
R5	4,06	4,03	4,02	-
R6	-5,50	-6,82	-7,72	-

As mentioned above, the prebarrier complex plays a fundamental role in the mechanism for the hydrogen abstraction; hence, the energy difference between the prebarrier complex and the isolated reactants is of great importance for the determination of the rate coefficients. The electronic energy differences between the prebarrier complex and the reactants, calculated at the CCSD/ACCD and CCSD(T)/CBS levels, are -5.00 and -5.15 $kcal \cdot mol^{-1}$, respectively. The inclusion of the zero point energy caused an increase of 1.84 $kcal \cdot mol^{-1}$.

In Figure 3, Gibbs free energy profiles for the formation of the prebarrier complex are shown for different temperatures. As can be seen from this Figure, thermal effects destabilize the prebarrier complex and, for temperatures above 400 K, the formation of the prebarrier complex becomes an endergonic process.

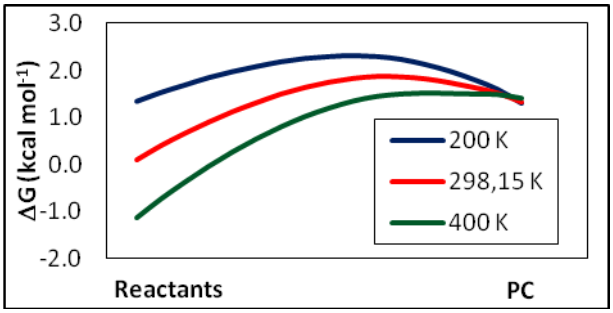

Figure 3: Gibbs free energy profiles for the formation of the prebarrier complex, at different temperatures.

Therefore, for temperatures below 400 K, a chemical model of the reaction R1 consisting of three elementary reactions was adopted:

$$CH_2O + OH \xrightarrow{k_1} PC$$
$$PC \xrightarrow{k_{-1}} CH_2O + OH$$
$$PC \xrightarrow{k_2} HCO + H_2O$$

Besides the prebarrier complex relative energy, the barrier height, defined as the zero point energy corrected difference between the saddle point and the reactants, is also important to the reaction, and, as mentioned above, an agreement among all available literature values is not observed. Our calculated barrier height values are 1.06, -1.18 and -1.35 kcal·mol^{-1} at the CCSD/ACCD, CCSD(T)/ACCD and CCSD(T)/CBS levels, respectively, suggesting that this parameter is very sensitive to the level of theory. The trend observed for the barrier height values also agrees with the data available in the literature, the lowest values for the barrier heights being yielded by the more robust methods. The barrier height at the complete basis set limit is in good agreement with the value found by Xu et al. [14].

Energy values obtained at the complete basis set limit were finally employed on the calculation of the rate coefficients, by adopting the canonical variational transition state method. A potential curve with 20 points between the reactants and the PC, and the corresponding molecular properties, were used to calculate k_1 and k_{-1}, and another potential curve with 17 points (including the saddle point), and the corresponding molecular properties, were used to calculate k_2. The global rate coefficients have been finally calculated by adopting the steady state approximation:

$$k_g = \frac{k_1 \cdot k_2}{k_{-1} + k_2}, \quad T < 400K$$

For temperature values above 400 K, the model for R.1 presumes the elementary $H_2CO + OH \rightarrow HCO + H_2O$ reaction, thus reactants are connected to the products passing through the saddle point. The rate coefficients were evaluated using the canonical variational transition state method with the same potential curve used to calculate k_2 in the previous situation, at low temperatures.

The rate coefficients, for both temperature ranges, are shown in Figure 4. It can be noted that at low temperatures the rate coefficients have a negative dependence with the temperature, which is caused by the destabilization of the PC with the increase of the temperature, in other words, the elementary reaction of dissociation of the PC into the reactants becomes more important as long as the temperature increase. The non-Arrhenius behavior remains at high temperatures up to 550 K, after that the rate coefficients are shown to increase with the increase of the temperature. From the values of rate coefficients calculated at low and high temperature ranges, the Arrhenius parameters have been estimated, and are expressed below (in units of cm^{-3} molec^{-1} s^{-1} and kcal·mol^{-1}):

$$k_1 = 5.76 \cdot 10^{-12} e^{\left(\frac{0.57}{RT}\right)}, \quad 200\ K < T < 400\ K$$

$$k_1 = 2.09 \cdot 10^{-7} \left(\frac{T}{298}\right)^{2.32} e^{\left(\frac{2.22}{RT}\right)}, \quad 400\ K < T < 2000\ K$$

It is noteworthy that the rate coefficients obtained for the high temperature range fit very well with the experimental values of Vasudevan *et. al* [15], indicating that the theoretical model used can accurately describe the experimental phenomena at high temperatures. At low temperatures, although the theoretical model supports the non-Arrhenius behavior, a fair quantitative agreement with the experimental data [7] is observed, with deviations of 35-129%.

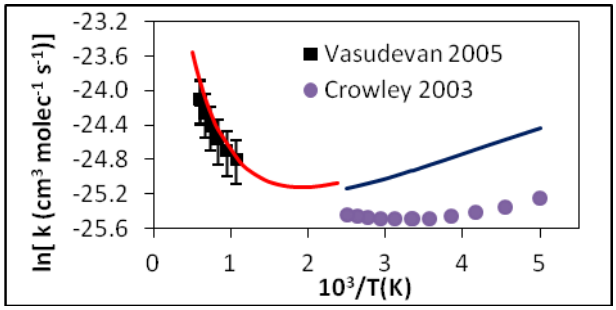

Figure 4: Calculated and experimental rate coefficients for the H abstraction reaction ($CH_2O+OH \rightarrow HCO+H_2O$) as function of the temperature.

The dissociation reaction of the formyl radical (R2), unlike most dissociation reactions for closed shell molecules, shows a saddle point, as can be seen in the reaction profile introduced in Figure 5. This type of potential curve for the formyl dissociation is supported

in the literature [24]. In this work, the saddle point has been found at 21.26 kcal mol^{-1} above de formyl radical at the level CCSD/ACCD. After the inclusion of the triples excitations, this value slightly decreases, while the extrapolation to the complete basis set limit the energy difference increases to 22.08 kcal mol^{-1}, as exhibited in Figure 5.

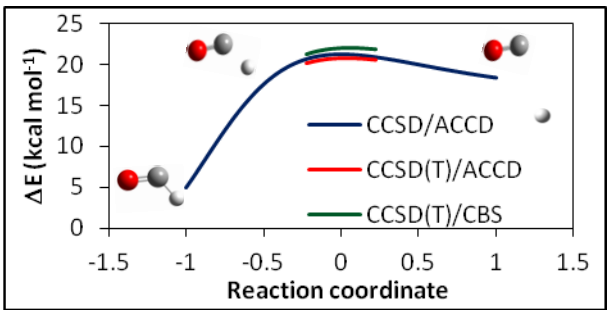

Figure 5: Reaction profile for the dissociation reaction of the formyl radical (HCO→H+CO).

The kinetics of the formyl dissociation reaction have been largely studied, but in most of the cases, in the low-pressure limit, in which the bath gas plays a fundamental role and the reaction follows a second order kinetics [25-27]. Since this condition has been extensively covered, we have focused on the evaluation of kinetic parameters only in the high pressure limit. In order to calculate the rate coefficients by the canonical variational transition state method, a potential curve with 21 points (including the saddle point), and the corresponding molecular properties were used. The rate coefficients show an Arrhenius behavior, with the parameters $1.21x10^{14}$ s^{-1} and 18.76 $kcal \cdot mol^{-1}$.

The reaction profile for the OH addition reaction to the formyl radical (R3), yielding the E conformer of the formic acid, was estimated by a Morse potential. For the potential curve, the distance between the carbon and the oxygen of the hydroxyl group was assumed as the reaction coordinate and increased, from the distance calculated for the formic acid at the CCSD/ACCD level, 1.355 Å, to 8.155 Å. A total of 35 points were calculated. The parameters in the Morse equation, necessary to calculate the energy values along the reaction coordinate, were $\Delta E = 115.13$ $kcal \cdot mol^{-1}$ and $\alpha = 1.3179$ $Å^{-1}$, ΔE corresponding to the energy difference of the reaction at the CCSD(T)/CBS level of theory. The parameters used for estimating the vibrational frequencies varied depending on the vibrational mode, whether it is conserved or lost along the reaction coordinate.

Variational rate coefficients for the the HCO + OH association, k_3, and for the (E)-CH_2O_2 dissociation (the reverse reaction, $k_{3,rev}$) have been calculated and are shown in Figure 6. The rate coefficients for the association reaction, k_3, are almost constant for the temperature range between 298K-1000K, with parameters -2.10 $kcal \cdot mol^{-1}$ and $9.13x10^{-9}$ $cm^3 \cdot molec^{-1} \cdot s^{-1}$, while the dissociation reaction ($k_{3,rev}$) presents a typical behavior, with the parameters 106.60 $kcal \cdot mol^{-1}$ and $1.93x10^{19}$ s^{-1}, valid in the same temperature range.

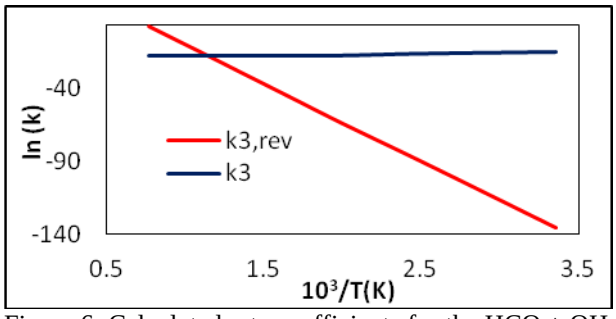

Figure 6: Calculated rate coefficients for the HCO + OH association (k_3), and for the (E)-CH_2O_2 dissociation ($k_{3,rev}$) as a function of the temperature.

It is assumed that the (E)-CH_2O_2, formed through R3, can dissociate via R3,rev or decompose via R4 or isomerize via R5, the latter yielding the (Z)-CH_2O_2 conformer, which further decomposes via R6. The barrier heights are: 65.03, 11.37 and 65.40 $kcal \cdot mol^{-1}$ for the (E)-CH_2O_2 decomposition reaction (R4), the (E)-CH_2O_2 → (Z)-CH_2O_2 isomerization and the (Z)-CH_2O_2 decomposition reaction (R6), respectively, at the CCSD(T)/CBS level of theory.

Similar variational procedures have been adopted for the calculation of the rate coefficients for the R4, R5 and R6 reactions. We note that, for the R4 reaction, the decomposition of (E)-CH_2O_2, two saddle points with the same energy were located, one being the specular image of the other. Due to the stereochemistry of the saddle point, rate coefficients have been multiplied by 2.

As can be seen in Figure 7, the rate coefficients for the decomposition reactions both (E) and (Z) formic acid conformers show an Arrhenius behavior, and the rate coefficients values are quite similar, which could be expected since the barrier height of both of them are approximately equal.

The Arrhenius parameters estimated for the (E)-CH_2O_2 → H_2O + CO reaction are 68.36 $kcal \cdot mol^{-1}$ and $1.27x10^{15}$ s^{-1}. For the (Z)-CH_2O_2 → H_2 + CO_2 reaction, the following Arrhenius parameters are suggested: 63.28 $kcal \cdot mol^{-1}$ and $3.25x10^{13}$ s^{-1}. These Arrhenius parameters are valid from 200 K to 2200 K.

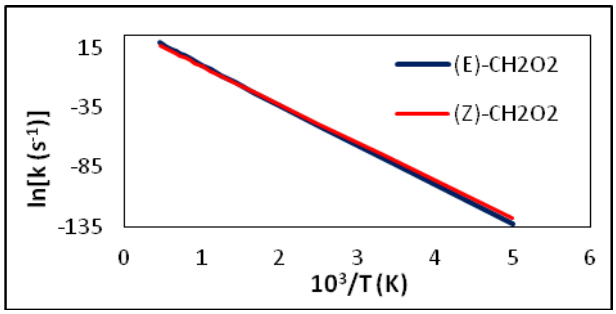

Fig 7: Calculated rate coefficients for the (E)-CH_2O_2 → CO + H_2O and (Z)-CH_2O_2 → H_2 + CO_2 reactions as a function of the temperature.

The comparison of theoretical and experimental rate coefficients values has not been possible, since most experiments have been conducted in the low pressure limit or fall-off region and only high-pressure rate coefficients have been predicted in this work. The experimental studies have reported that the (E)-CH_2O_2 → H_2O + CO reaction is the preferred decomposition channel [28,29]. This fact can be explained by the isomerization reaction: up to 2200 K, the rate coefficient of formation of the E conformer ($k_{5,rev}$) is, at least, twice the value of the rate coefficient for the formation of the Z conformer (k_5), as can be seen from Figure 8. The estimated Arrhenius parameters for (E)-CH_2O_2 → (Z)-CH_2O_2 isomerization are 12.04 kcal·mol^{-1} and 2.06x10^{13} s^{-1} and, for the reverse reaction, 7.98 kcal·mol^{-1} and 1.70x10^{13} s^{-1}.

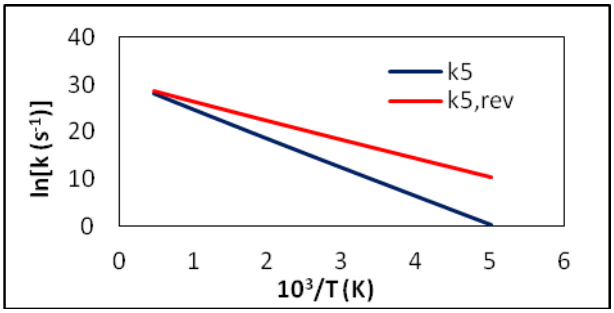

Figure 8: Calculated rate coefficients for the isomerization reactions (k_5: (E)-CH_2O_2 → (Z)-CH_2O_2 and $k_{5,rev}$: (Z)-CH_2O_2 → (E)-CH_2O_2) as a function of the temperature.

The Arrhenius parameters for all elementary reactions involved in the proposed mechanism for formaldehyde oxidation are summarized in Table 2.

Table 2: Arrhenius parameters for all elementary reactions involved in the proposed mechanism for formaldehyde oxidation. Activation energies are given in kcal.mol^{-1} and temperature values in K. The pre-exponential factors are given in s^{-1} or cm^3 molecule^{-1} s^{-1} (see footnotes).

Reaction	A	n	Ea	Temp.
R1[(b)]	2.09x10^{-7}	0	0.57	200-400K
R1[(b)]	3.80x10^{-13}	2.32	2.22	400-2000K
R2[(a)]	1.21x10^{14}	0	18.76	200-2200K
R3[(b)]	9.13x10^{-9}	0	-2.10	298-1300K
R3[(a)] (reverse)	1.93x10^{19}	0	106.60	298-1300K
R4[(a)]	1.25x10^{15}	0	68.36	200-2200K
R5[(a)]	2.06x10^{13}	0	12.04	200-2200K
R5[(a)] (reverse)	1.70x10^{13}	0	7.98	200-2200K
R6[(a)]	3.25x10^{13}	0	63.28	200-2200K

(a) Reactions R2, R3rev, R4-6 are first-order and the pre-exponential factor are given in s^{-1}.
(b) Reactions R1 and R3 are second-order and the pre-exponential factor are given in cm^3 molecule^{-1} s^{-1}.

With all calculated rate coefficients, the concentration profiles for the species involved in the proposed chemical model were obtained, as a function of time, under atmospheric and combustion conditions. To simulate the atmospheric conditions, the temperature was set at 298 K, the initial concentrations of formaldehyde and hydroxyl radicals (constant value) were 4.01x10^6 and 5x10^6 molec·cm^{-3}. For the simulation at combustion condition, the temperature set as 1000 K and the concentrations of formaldehyde (constant value) and hydroxyl radicals were: 4.01x10^{11} and 5x10^6 molec·cm^{-3}.

In order to solve all coupled differential equations, the software Kintecus® has been used. The results of the simulation at atmospheric conditions are exhibited in Figure 9. From this Figure, it can be seen that the concentrations of atomic hydrogen, carbon monoxide and (E)-CH_2O_2 are approximately equal, at all time values, suggesting that, for this condition, the reactions R2 and R3 are the most important for the termination of the mechanism.

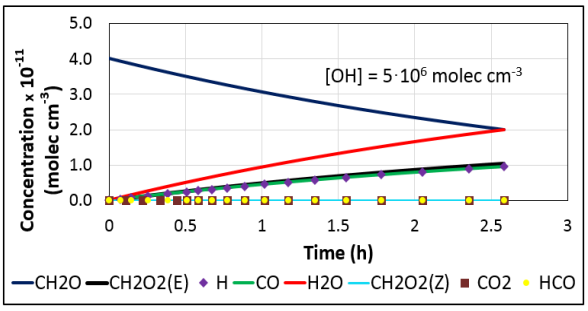

Figure 9: Concentration profiles for the species, as a function of time, at atmospheric condition (T=298K).

The results for the simulation at the combustion conditions are shown in Figure 10. It can be observed from this Figure that the concentrations of water, atomic hydrogen and carbon monoxide are approximately the same, indicating that the water is produced only from the reaction R1 and the hydrogen and carbon monoxide are from the R3, also suggesting that, at this temperature, formyl radicals are too unstable, decomposing through reaction R3, prior to react with the hydroxyl radicals.

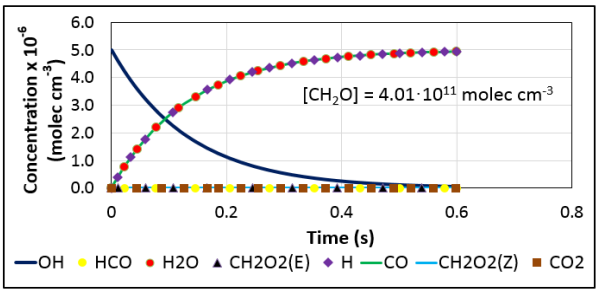

Figure 10: Concentration profiles for the species, as a function of time, at combustion condition (T=1000 K).

Conclusions

In this work, a chemical model for formaldehyde oxidation, initiated by hydroxyl radicals was revisited, due to the large discrepancy on the previous theoretical studies for the reaction of hydrogen abstraction (CH_2O+OH→HCO+H_2O), since we noted that the most

robust levels of theory applied have given the lowest barrier height for this reaction. Moreover, it was also observed that there are a significant number of papers of the reactions of decomposition of the formyl radical and the formic acid at the low pressure or fall off reaction, but there was a lack of information about the high pressure limit. Hence, a mechanism involving these species was assessed in the high pressure limit at CCSD(T)/CBS level of theory. The trend observed for the barrier height of the formaldehyde hydrogen abstraction was confirmed in this work, and the results are in good agreement with the most recent works. Therefore, to the best of our knowledge, the procedure adopted was good enough to characterize quantitatively the energetic profile of the mechanism.

The rate coefficients of all elementary reactions have been calculated adopting a canonical variational transition state method, for a large range of temperature (200-2200K). Then it was possible to clarify the change in the mechanism of hydrogen abstraction, which follows a non-Arrhenius behavior at low temperatures and the typical behavior at high temperatures. This fact was attributed to the destabilization of the prebarrier complex for temperatures above 400 K. Furthermore, the principal via of decomposition of the formic acid, yielding carbon monoxide and water instead of carbon dioxide and molecular hydrogen, which is well known by previous experimental works, have been attributed to the preferential via of isomerization, from the Z conformer to the E.

Finally, with the values of rate coefficients, two simulations of the behavior of the species in the mechanism have been done, one at atmospheric condition (298 K) and the other at combustion condition (1000 K), where have been found that at atmospheric condition the main pathways of termination of the mechanism are the decomposition of the formyl radical and the formation of the E conformer of the formic acid, while at combustion condition the main via is only the decomposition of the formyl radical.

Acknowledgements

The authors thank CAPES and FAPERJ (E-26/010.003338/2014) for the financial support to this project.

References

[1] M.C. Rodrigues, L.L.N. Guarieiro, M.P.Cardoso, L.S. Carvalho, G.O. da Rocha, J.B. de Andrade, Fuel 92 (2012) 258-263

[2] D.J. Luecken, W.T. Hutzell, M.L. Strum, G.A. Pouliot, Atmos. Environ. 47 (2012) 477-490

[3] B.B. Guven, E.P. Olaguer, Atmos. Environ. 45 (2011) 4272

[4] J. Zheng, R. Zhang, J.P. Garzón, M.E. Huertas, M. Levy, Y. Ma, R. Torres-Jardón, L.G. Ruiz-Suárez, L. Russel, S. Takahama, H. Tan, G. Li, L.T. Molina, Atmos. Environ. 70 (2013) 513-520.

[5] S.M. Corrêa, G. Arbilla, E.M. Martins, S.L. Quitério, C.S. Guimarães, L.V. Gatti, Atmos. Environ. 44 (2010) 2302-2308

[6] B. D'Anna, V. Bakken, J.A. Beukes, C.J. Nielsen, K. Brudnik, J.T. Jodkowski, Phys. Chem. Chem. Phys. 5 (2003) 1790-1805

[7] V. Sivakumaram, D. Hölscher, T.J. Dillon, J.N. Crowley, Phys. Chem. Chem. Phys. 5 (2003) 4821-4827

[8] J.R. Alvarez-Idaboy, N. Mora-Diez, R.J. Boyd, A. Vivier-Bunge, J. Am. Chem. Soc. 123 (2001) 2018-2024

[9] R. Atkinson, J.N. Pitts Jr., J. Chem. Phys. 68 (1978) 3581-3584

[10] M. Dupuis, W.A. Lester Jr., J. Chem. Phys. 81 (1984) 847-850

[11] J.S. Francisco, J. Chem. Phys. 96 (1992) 7597-7602

[12] M.R. Soto, M. Page, J. Phys. Chem. 94 (1990) 3242-3246

[13] H.Y. Li, M. Pu, Y.Q. Ji, Z.F. Xu, W.L. Feng, Chem. Phys. 307 (2004) 35-43

[14] S. Xu, R.S. Zhu, M.C. Lin, Int. J. Chem. Kin. 5, 38 (2006) 322-326

[15] V. Vasudevan, D.F. Davidson, R.K. Hanson, Int. J. Chem. Kin. 2, 37 (2005) 98-109

[16] Y. Zhao, B. Wang, H. Li, L. Wang, THEOCHEM 818 (2007) 155-161

[17] S. Wang, D.F. Davidson, R.K. Hanson, Proc. Comb. Inst. 35 (2015) 473-480

[18] K.A. Fukui, J.Phys. Chem 74 (1970) 4161-4163

[19] L.A. Curtis, J.E. Carpenter, K. Raghavachari, J. Pople, A. J. Chem. Phys. 96 (1992) 9030-9034

[20] R.H. Nobles, W.J. Bouma, L. Radom, Chem. Phys. Lett. 89 (1982) 497-500

[21] S. Vandresen, S.M. Resende, J. Phys Chem. A 108 (2004) 2284-2289

[22] J.C. Ianni, Computational Fluid and Solid Mechanics (2003) 1368-1372

[23] NIST Computational Chemistry Comparison and Benchmark Database, NIST Standard Reference Database Number 101, Realease 16a, August 2013, Editor: Russell D. Johnson III, available in http://cccbdb.nist.gov/

[24] S.W. Cho, W.L. Hase, J. Phys. Chem. 94 (1990) 7371-7377

[25] H. Hippler, N. Krasteva, F. Striebel, Phys. Chem. Chem. Phys. 6 (2004) 3383-3388

[26] L.N. Krasnoperov, E.N. Chesnokov, H. Stark, A.R. Ravishankara, Proc. Combust. Inst. 30 (2005) 935-943

[27] J. Li, Z.W. Zhao, A. Kazakov, M. Chaos, F.L. Dryer, J.J. Scire, Int. J. Chem. Kinet. 39 (2007) 109-136

[28] K. Saito, T. Shiose, O. Takahashi, Y. Hidaka, F. Aiba, K. Tabayashi, J. Phys. Chem A 109 (2005) 5352-5357

[29] A. Elwardany, E.F. Nasir, Et. Es-sebbar, A. Farooq, Proc. Comb. Inst. 35 (2015) 429-436